Corrosive wear behaviour of various stainless steel alloys and a Stellite 6 weld cladding

F.Brownlie[1*], T.Hodgkiess[2], A.Pearson[3], A.M.Galloway[1]

[1]*Department of Mechanical & Aerospace Engineering, University of Strathclyde, Glasgow, UK.*

[2]*Porthan Ltd, Lochgilphead, UK.*

[3]*Weir Engineering Services, East Kilbride, UK*

Abstract

This study has comprised an investigation the corrosive wear behaviour of UNS S31600, a low hardness (280Hv) UNS S42000, a high hardness (480Hv) UNS S42000 and a single layer Stellite 6 (UNS R30006) weld cladding on a low alloy carbon steel (UNS G43400). Erosion-corrosion testing was conducted using a submerged jet of 3.5% NaCl aqueous solution with spherical silica sand particles. The sand concentration was 2.4g/l, the velocity of the jet was 18m/s and the testing temperature range was 16°C-27°C. Both normal incidence (90°) and low angle (20°) tests were performed. Mass losses, wear scar depths and a volumetric analysis technique were used to assess the damage in the direct impinged zone (DIZ) and the outer area (OA) of the specimens. For all materials, it was found that mass loss was higher at 20° tests than that of 90°. However, when comparing wear scar depths the opposite trend was found. The results are discussed in terms of comparative material behaviour, the influence of material hardness and the corrosive wear mechanisms in different regions formed during slurry jet impingement.

Keywords: Erosion-corrosion, impingement, volumetric analysis

*Corresponding author: Frazer Brownlie (f.brownlie@strath.ac.uk).

1. INTRODUCTION

Erosion-corrosion is an intricate material degradation process which involves mechanical wear, electrochemical processes and the combined effect of both, termed synergy. This material deterioration phenomenon is often a major issue for engineering components such as pump impellers, casings, pipework and mechanical seals. The destructiveness of erosion-corrosion regularly results in loss of equipment efficiency and has the potential to result in catastrophic failures leading to extensive maintenance downtime and repair. To minimise the risk of failures there are two crucial factors which must be considered. Firstly, it is important to fully comprehend the environment in which the component is operating. The second vital factor is material selection.

One method of reducing the impact of erosion-corrosion is to use Corrosion Resistant Alloys (CRAs). These are a group of materials that form passive oxide films which provide a thin protective layer against corrosion. Austenitic and martensitic stainless steels, such as SS316 (UNS S31600) and SS420 (UNS S42000), are prime examples of CRAs which are commonly used in engineering applications. Another such example is Stellite 6 (UNS R30006) which consists of a cobalt based matrix with chromium carbide hard phases which is used broadly in applications where components experience erosive and corrosive environments.

As the austenitic stainless steel, SS316, is used extensively in engineering components, its erosion-corrosion characteristics have been well reported. Studies using a slurry pot testing method by Rajahram et al. [1–3] found that material removal of the stainless steel alloy was caused by either cutting or ploughing and subsequently lip removal. A network of subsurface cracks was also found after testing, the formation of these cracks was attributed to material phase transformation from austenite to martensite. This phase transformation is caused by the work hardening of the surface as it is impacted repeatedly by the hard sand particles [4]. A comparative study using an impinging jet erosion-corrosion technique, found that SS316 and SS420 behaved similarly in terms of both mass loss and wear scar depths. This was again attributed to the phase transformation of the austenitic stainless steel [5].

The wear resistance of Stellite 6 has also been studied in the past. Cast Stellite 6 and Hot Isostatically Pressed (HIPed) Stellite 6 has been found to have better erosion-corrosion resistance than SS316 [6–8]. This was due to the complexity of the Stellite 6 microstructure which contains a Cobalt matrix with a dendritic carbide structure. Another study by Romo et al. [9] investigated the slurry erosion resistance of a Shielded Metal Arc Weld (SMAW) Stellite 6 weld cladding compared to a 13Cr-4Ni stainless steel. The slurry consisted of tap water and silica sand particles and in short-term (5 minutes) tests. Stellite 6 exhibited better erosion resistance than the stainless steel at all impingement angles. These studies indicate that the basic erosion-corrosion behaviour of Stellite 6 material compared well with that of stainless steels and that a weld cladded Stellite 6 may be a useful option for a surface coating on a less resistant substrate.

The effect of the angle at which the sand particles impact the surface is also an important aspect to consider as the sand may impact an engineering component at numerous angles depending on the shape of the component and operating conditions. Zhao et al. found that the mass loss of SS316 increased with decreasing the impact angle [10]. Burstein et al. used a slurry jet with an acoustic emission technique to discover that sharp rises in current indicated that the oxide film of a SS304 alloy was penetrated. It was also observed that the current increased with decreasing the angle of impact and hence, synergy was found to be enhanced at lower angles [11]. The effect of impact angle of Stellite 6 and SS316 has also been studied [12]. This study found that the SS316 mass loss increased with decreasing impact angle and that Stellite 6 did not respond in a simple ductile or brittle manner. An investigation into the effect of impact angle on SS420 found that severe material degradation occurred at both grazing (30°) and normal (90°) incidence angles [13].

This study has investigated the erosion-corrosion performance of a SS316, SS420 (low hardness and high hardness) and a Hot Wire Tungsten Inert Gas (HWTIG) Stellite 6 weld cladding. An impingement slurry jet technique was used and materials were tested at 20° and 90° angles of impingement. The tested materials were assessed in terms of mass loss, wear scar depths and a recently developed in-house volumetric analysis technique [14].

2. MATERIALS AND METHODS

2.1 Materials under study

The materials investigated in this study were SS316, low hardness (LH) martensitic SS420, high hardness (HH) martensitic SS420 and a single layer Stellite 6 weld cladding of thickness 1.5mm. The SS316 was used as a reference material. Table 1 illustrates the nominal chemical composition of each of the materials.

Table 1: *Chemical composition for the stainless steels and Stellite 6 weld cladding*

Material	C%	W%	Cr%	Ni%	Mo%	S%	Mn%	Si%	N%	Fe%	Co%
SS316	0.08	-	17.5	12	2.5	<0.03	<2	<0.75	<0.1	Bal.	-
SS420	<0.15	-	13	-	-	<0.03	<1	<1	-	Bal.	-
Stellite 6 weld cladding	<1.4%	4.7	24.8	-	0.08	-	1.1	0.9	-	18.9	Bal.

The higher hardness of 480HV for the martensitic SS420 was obtained through a heat treatment process. Samples of the LH SS420 were austenised at a temperature of 1000°C for a minimum period of 1 hour and were then oil quench hardened. The samples were then tempered at a temperature of 250°C for a minimum of 1 hour and were then cooled to room temperature. The welding process used to produce the Stellite 6 weld cladding samples was HWTIG. An Olympus GX51 microscope was used to examine the microstructure of each of the materials prior to testing. The materials were polished to 3µm diamond and etched in either Kallings reagent (SS420), Murakami's reagent (Stellite 6) or electrolytic etching in 10% oxylic acid (SS316). Figures 1-4 demonstrate the microstructure for each of the tested materials.

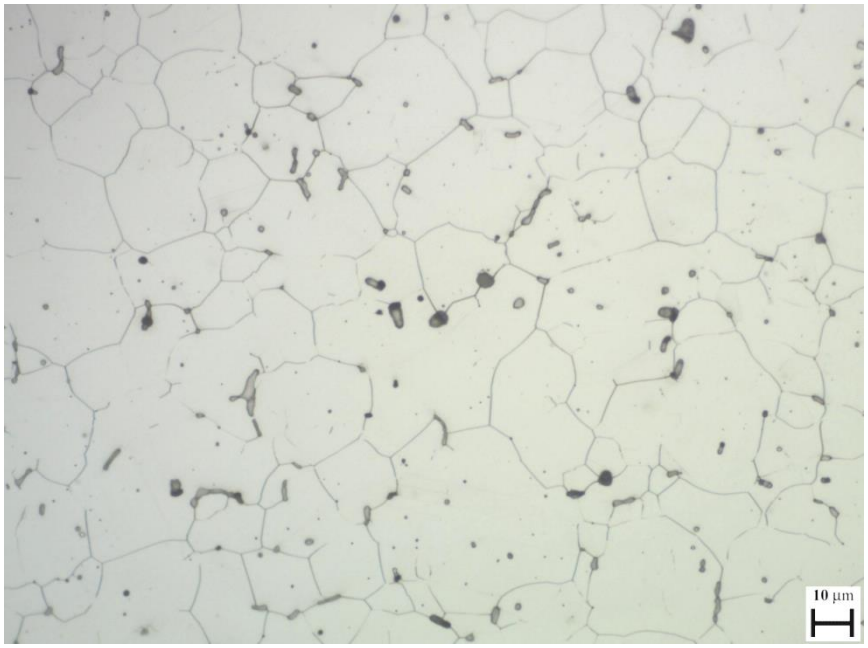

Figure 1: *SS316 microstructure demonstrating typical austenitic grain structure with δ-ferrite located at grain boundaries (seen as dark spots)*

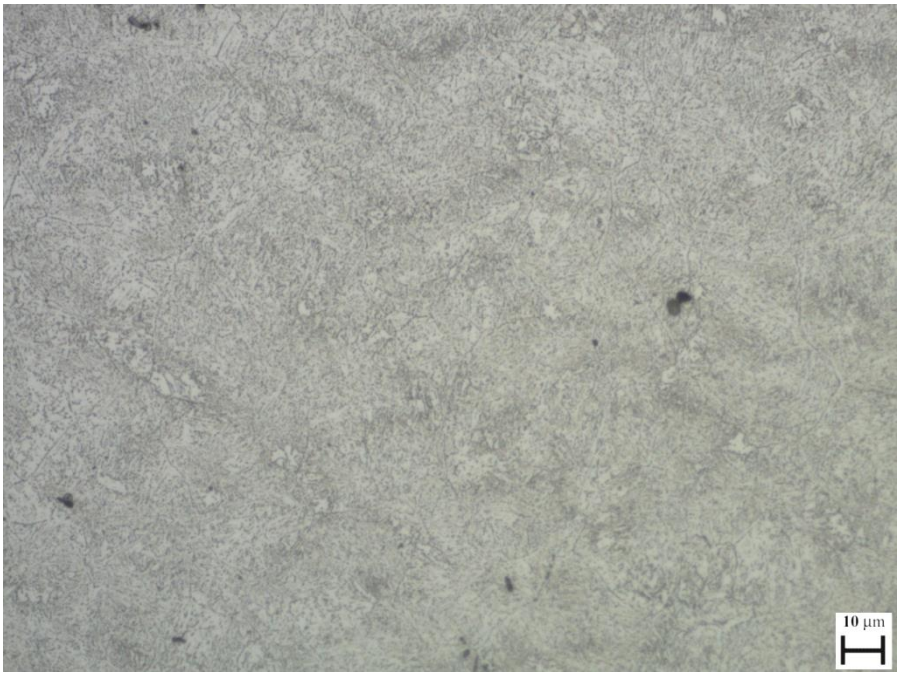

Figure 2: *LH SS420 microstructure demonstrating tempered martensite*

Figure 3: *HH SS420 microstructure demonstrating tempered martensite*

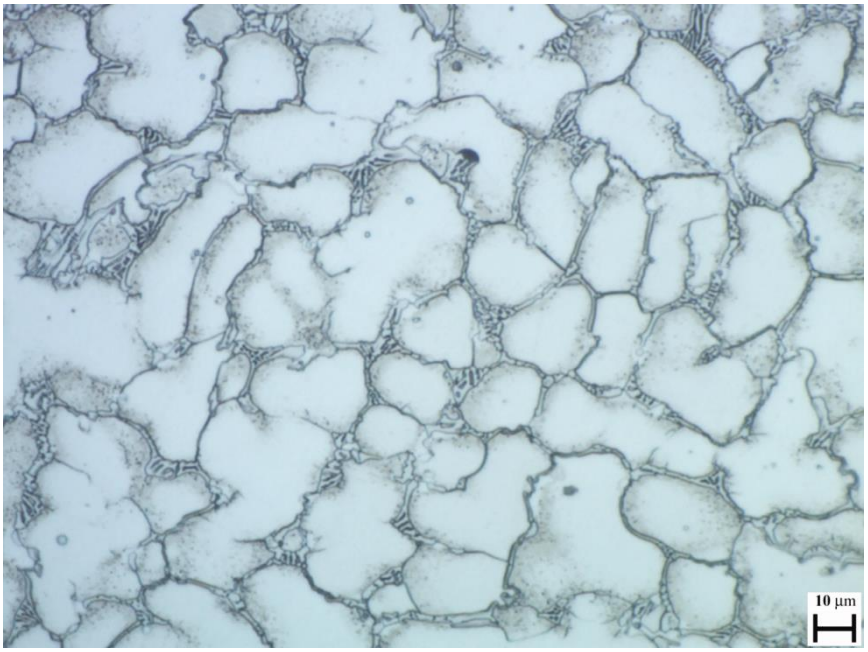

Figure 4: *Stellite 6 microstructure consists of Co-rich dendrites surrounded by Cr-rich, M_7C_3, eutectic carbides in a solid solution cobalt matrix*

A macro-hardness testing machine, with a 5 kgf load was used to measure the hardness values of each of the materials, shown in Table 2.

Table 2: *Hardness values for each of the materials*

Material	SS316	LH SS420	HH SS420	Stellite 6 weld cladding
Hardness (HV)	200	280	480	400

2.2 Testing apparatus

The erosion-corrosion testing apparatus consists of a closed loop recirculating system, as shown in Figure 5. Tests were conducted with a submerged jet of 3.5%NaCl aqueous solution with suspended spherical silica sand of 2.4g/l concentration. The velocity of the jet was 18m/s with a testing temperature range of 16°C-27°C. Tests were conducted at two angles, normal incidence (90°) and a shallow angle (20°). Experiments were conducted for 1 hour. The diameter of the nozzle was 3.8mm. All samples were round with a diameter of 38mm. The distance between the nozzle and sample was kept at 5mm to ensure consistency in results. Examples of the typical wear scar at both angles are shown in Figures 6-7. The silica sand size distribution is shown in Table 3.

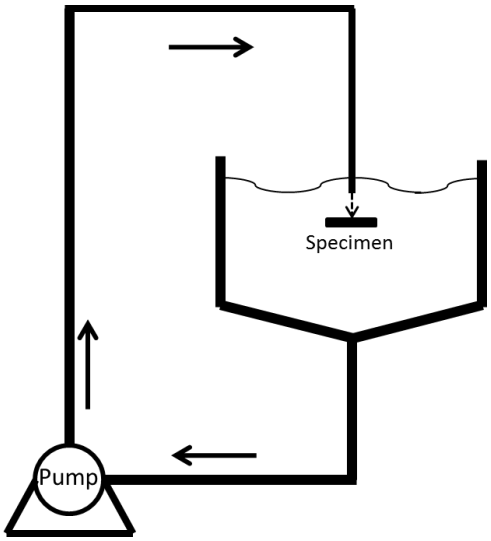

Figure 5: *Schematic of erosion-corrosion rig*

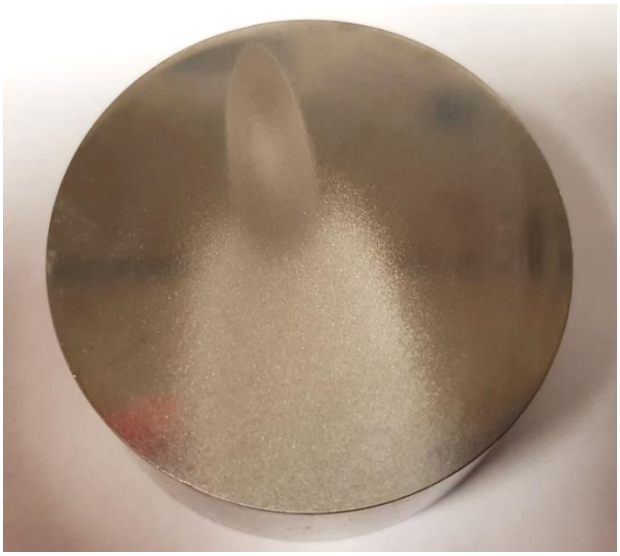

Figure 6: *Wear scar on SS316 after 1hr test at 20° impingement*

Figure 7: *Wear scar on SS316 after 1 hr test at 90° impingement, highlighting the two distinct wear zones*

Table 3: *Sand size distribution*

Size (µm)	≤ 250	250-420	421-500	501-600	≥ 601
Percentage (%)	2.5	18.4	50.7	23.3	5.1

A mass balance with accuracy of ±0.1mg, was used to measure the mass losses occuring after each erosion-corrosion test. Wear scar depths and volume losses were measured by using an Alicona Infinite Focus 3D measurement scanner.

3. RESULTS

3.1 Total mass losses

The overall erosion-corrosion performance of the tested materials was assessed by evaluating the total mass losses after each test. A minimum of four replicates of each material at both impingement angles was conducted. Figure 8 shows the average mass losses for each test material at both impingement angles.

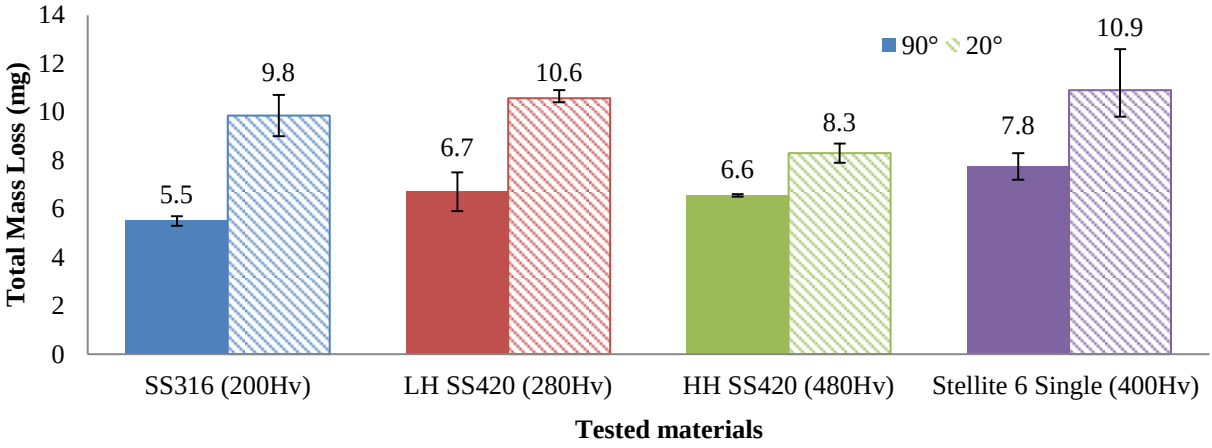

Figure 8: *Average mass losses for test materials at both impingement angles*

Comparison of the mass losses between the impingement angles conveys a distinct increase in mass loss from 90° to 20° impingement tests. At 90° impingement, the SS316 was found to have the lowest mass loss. However, at 20° the high hardness martensitic SS420 had the lowest mass loss. The Stellite 6 weld cladding exhibited the largest average mass loss at both impingement angles.

3.2 Surface topography

3.2.1 Wear scar depths

Erosion-corrosion performance was also assessed by evaluating wear scar depths (under the direct impinged zone). For each specimen several measurements were taken in order to identify the deepest wear scar depth. Figure 9 demonstrates a typical U-shaped wear scar of a Stellite 6 weld cladding sample.

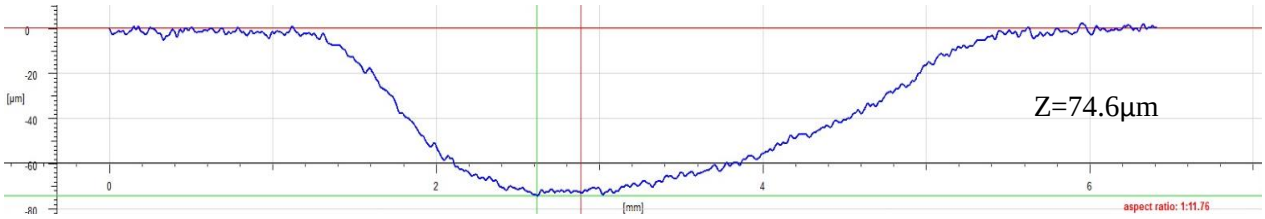

Figure 9: *Wear scar of a Stellite 6 weld cladding*

Figure 10 illustrates the average wear scar depths for the tested materials at both angles of impingement.

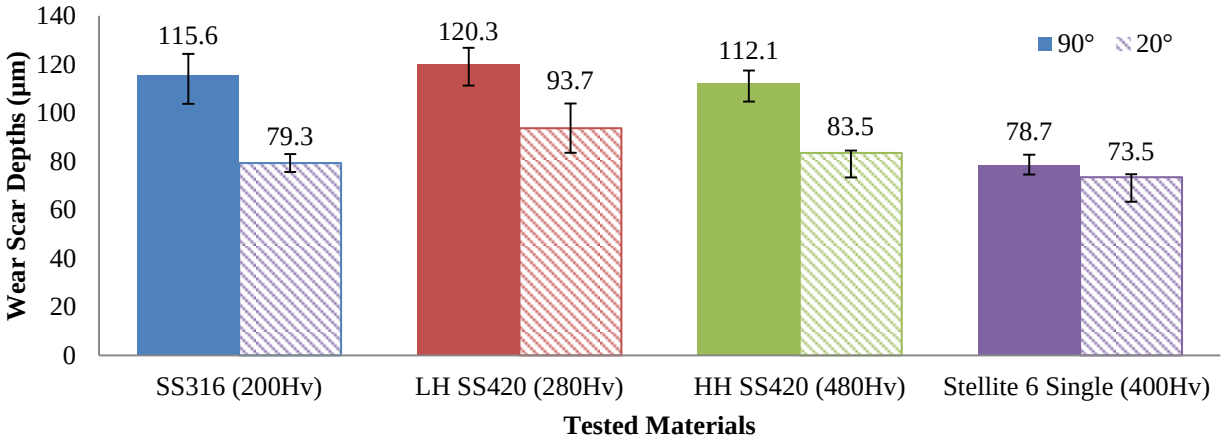

Figure 10: *Average wear scar depths for the materials at both impingement angles*

Wear scar depth measurements demonstrated that the wear scars were generally deeper in tests conducted at 90° impingement than these involving 20° angle. The Stellite 6 weld cladding demonstrated the lowest wear scar depths at both impingement angles. When comparing the average wear scar depth of the Stellite 6 weld cladding against the other tested materials, there was a 30-35% reduction in wear scar depth at 90° angle of impingement and a 7-22% reduction in wear scar depth at 20° impingement angle.

3.2.2 Volume loss measurements

As a 3D representation in the direct impinged zone (DIZ) was measured, then volume losses could also be obtained. This is additional information which can be used to assess the damage directly underneath the slurry jet. Figure 11 demonstrates a volume loss measurement scan of a Stellite 6 weld cladding specimen after a 90° impingement test. Figure 12 shows the volume losses for the LH and HH SS420 and Stellite 6 weld cladding. Volumetric analysis was not conducted on the SS316 as it was only used as a reference material. The Stellite 6 weld cladding demonstrated the lowest volume loss in the DIZ when compared to the martensitic stainless steels.

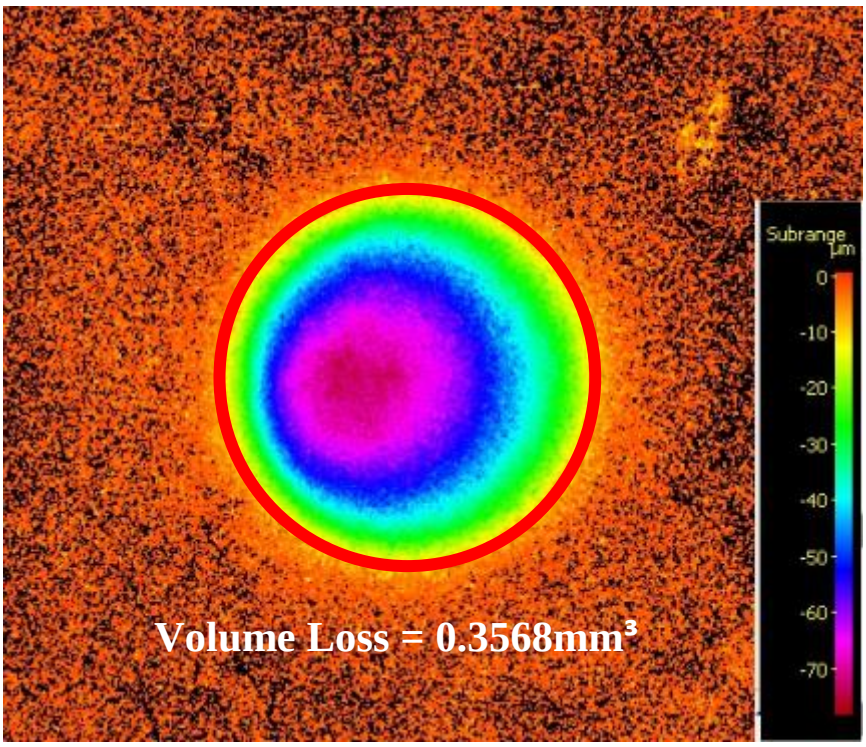

Figure 11: *Representation of volume loss measurement of Stellite 6 weld cladding at 90° impingement test*

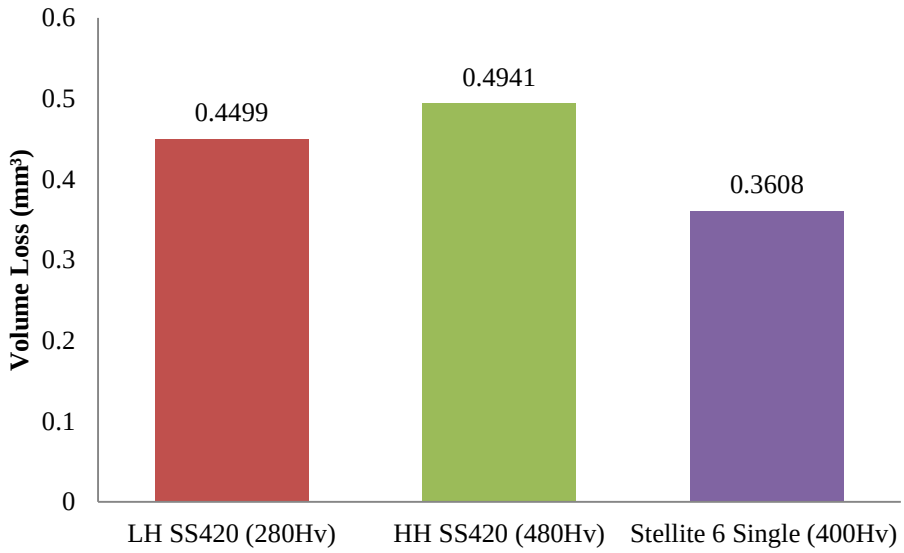

Figure 12: *Volume losses of materials after 90° impingement tests*

3.2.3 Mass losses in distinct zones

During the erosion-corrosion testing, there are two distinct wear regions which exist. The first region is formed directly underneath the impinged jet (DIZ) and the second is formed in an outer area (OA) outside the impinged zone. These zones can be visibly seen in Figure 6. As the total mass loss of the material is known and the volume loss in the DIZ is obtained, then it is possible to calculate the mass loss (via material density) in the DIZ and subsequently the mass loss in the OA [14].

Figure 13 illustrates the breakdown of the mass losses into the two wear regions formed during 90° impingement testing conditions. The martensitic stainless steels demonstrated the greatest mass losses in the DIZ, due to the large volume loss, however they demonstrated a relatively low mass loss in the OA. The Stellite 6 weld cladding demonstrated the opposite trend; it had the lowest mass loss in the DIZ but portrayed the largest mass loss in the OA.

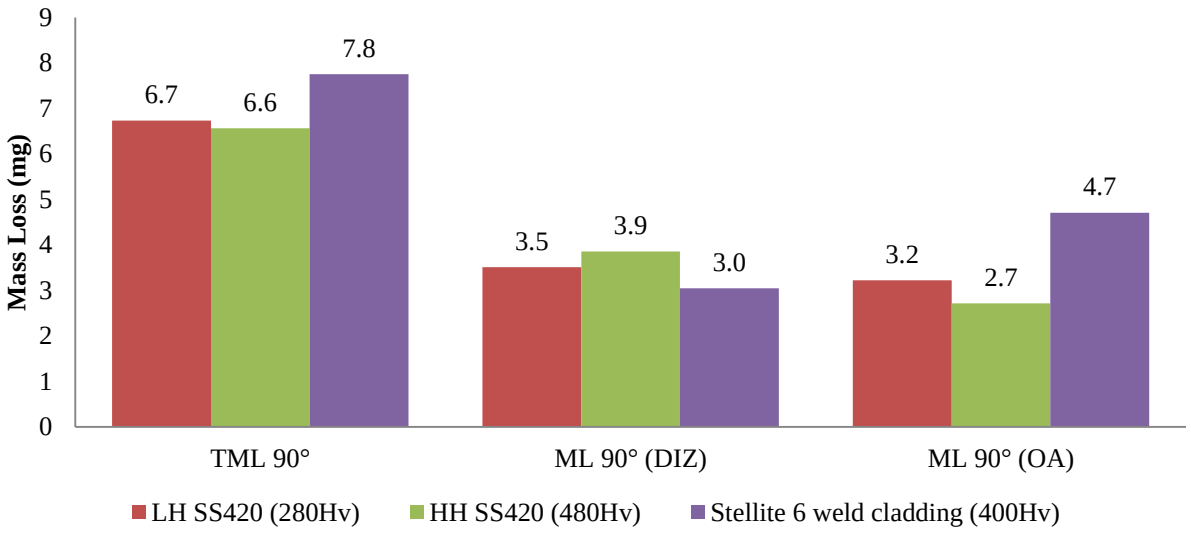

Figure 13: *Breakdown of mass losses in the two distinct wear regions in 90° impingement conditions*

4. DISCUSSION

From the total mass losses (Figure 7) it can be seen that all materials have greater mass losses under impingement at 20° than at 90°. Therefore, all materials are following the erosive ductile behaviour theory proposed by Finnie [15], despite their significant differences in hardness and any influence of corrosive processes. It should also be noted that materials have different microstructures apart from the SS420 samples. When comparing only the martensitic SS420 materials it is noticeable that the total mass loss at 90° impingement is similar, but at 20° impingement, the higher hardness SS420 has significantly less total mass loss. This indicates that the hardness for a martensitic microstructure is significant only at 20° impingement where the majority of the damage is low angle abrasion. The total mass loss of the Stellite material was the highest of all the materials tested at both impingement angles.

However, when comparing wear scar depths a different trend is found. These measurements indicate that the Stellite 6 weld cladding demonstrates the best direct impingement erosion-corrosion resistance of the tested materials at both impingement angles. There was a slight difference in the high and low hardness SS420 materials, but the wear scar depths were very similar indicating that there was not much difference between their performances in the DIZ. The SS316 had similar wear scar depths as the martensitic stainless steels. A reasonable explanation of this is local work hardening effects from the sand particles; which may also result in localised phase transformation from austenite to martensite [1,3,4,16].

When volume losses are compared, there is some linkage to hardness, with the Stellite 6 weld cladding having the lowest volume loss with the high hardness martensitic SS420 having the greatest volume loss and the LH SS420 being an intermediate. There is also some linkage with wear scar depths and volume losses with Stellite 6 demonstrating the smallest material loss in both cases. However, the link is not so apparent for the martensitic stainless steels. A reasonable explanation for this is that the volume loss is dictated not only by the depth but also the shape of the wear scar. Therefore, a deep wear scar does not necessarily equate to a large volume loss, as can be seen in Figure 14.

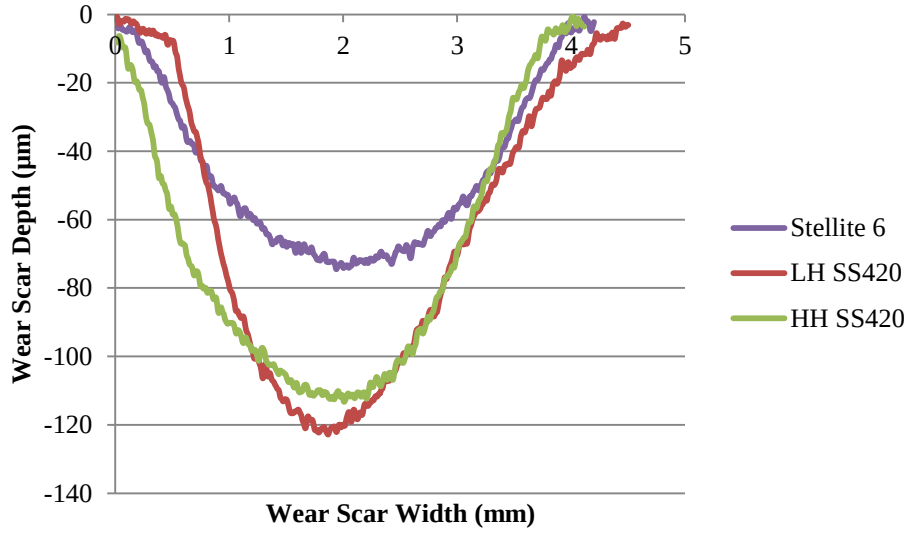

Figure 14: *Comparison of wear scar profile for each of the tested materials*

The mass losses in the distinct zones (Figure 12) indicate that the Stellite 6 weld cladding has a slightly better wear resistance in the DIZ but in the OA its performance is significantly worse than that of the two martensitic stainless steels. It is well known that sliding abrasion resistance increases with hardness [17,18]. This relationship is demonstrated by the two martensitic stainless steels in that the HH SS420 has a reduction in mass loss when compared to the LH SS420. The high material loss in the OA of the Stellite 6 weld cladding, however, does not seem to correlate with its relatively high hardness. It may be that the relatively high mass losses of the Stellite 6 weld cladding in the OA are associated with enhanced pure corrosion or corrosion-induced synergy - especially as a synergy mechanisms may be facilitated by the complex microstructure of the Stellite (Figure 4).

It is considered, however, that a contributing factor, in the relatively poor behaviour of the Stellite weld cladding in the OA, was the presence of welding defects such as inclusions (Figure 15), which were found on the surface of the Stellite 6 weld cladding. These defects will clearly hinder the material's corrosive wear performance. The inclusions were found to be Co-rich (approximately 94% Co) with a hardness of 200HV. This lower hardness and lower Chromium content would be likely to contribute to enhanced deterioration by both abrasive wear and corrosion mechanisms.

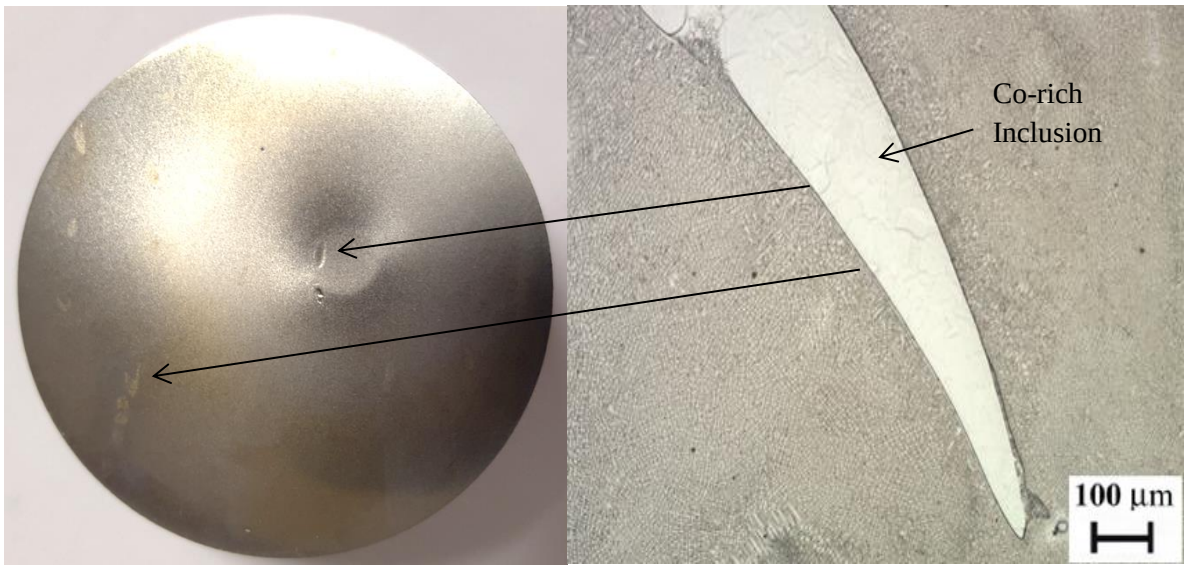

Figure 1: *Co-rich inclusion found on surface of Stellite 6 weld cladding*

In a general sense, Figure 13 clearly demonstrates how slurry jet tests that generate total mass loss data *alone* are likely to provoke interpretation of comparative material behaviour that is limited in scope and potentially

misleading in terms of the damage occuring in different regions of a component. This feature is clearly evident when comparing the performance of the Stellite weld cladding with the stainless steels in this study.

Observations from this study has indicated that a Stellite 6 weld overlay on a low grade substrate is capable of providing protection that would be associated with the behaviour of CRA's like stainless steels. Perhaps, not surprising, however, the quality of the weld cladding process is a crucial factor.

5. CONCLUSIONS

1) This study has shown the complexity of erosion-corrosion as a phenomena and importance of using a more comprehensive range of examination and analysis techniques to evaluate the corrosive wear performance of materials.

2) In terms of both total mass losses and wear scar depths, the austenitic stainless steel and the two martensitic stainless steels demonstrated similar erosion-corrosion performance, despite the diversity of both mechanical and chemical properties. This is attributed to the work hardening effect of the austenitic stainless steel.

3) The Stellite 6 weld cladding demonstrated relatively good erosion-corrosion resistance in direct impingement conditions underneath the jet; however, it exhibited relatively poor sliding abrasion/corrosion resistance in the outer area. This is likely to be associated with weld defects in the form of Co-rich inclusions.

4) Relative hardness is not a major factor in overall erosion-corrosion performance. However, it can be related with sliding abrasion resistance.

6. ACKNOWLEDGMENTS

The authors would like to acknowledge the support for this study, which was provided by the Weir Group PLC (WARC2011SAA1, 2011) via its establishment of the Weir Advanced Research Centre (WARC) at the University of Strathclyde.

7. REFERENCES

[1] S. S. Rajahram, T. J. Harvey, J. C. Walker, S. C. Wang, and R. J. K. Wood, "Investigation of erosion-corrosion mechanisms of UNS S31603 using FIB and TEM," *Tribol. Int.*, vol. 46, no. 1, pp. 161–173, 2012.

[2] S. S. Rajahram, T. J. Harvey, and R. J. K. Wood, "Erosion–corrosion resistance of engineering materials in various test conditions," *Wear*, vol. 267, no. 1–4, pp. 244–254, 2009.

[3] S. S. Rajahram, T. J. Harvey, J. C. Walker, S. C. Wang, R. J. K. Wood, and G. Lalev, "A study on the evolution of surface and subsurface wear of UNS S31603 during erosion-corrosion," *Wear*, vol. 271, no. 9–10, pp. 1302–1313, 2011.

[4] R. J. K. Wood, J. C. Walker, T. J. Harvey, S. Wang, and S. S. Rajahram, "Influence of microstructure on the erosion and erosion-corrosion characteristics of 316 stainless steel," *Wear*, vol. 306, no. 1–2, pp. 254–262, 2013.

[5] L. Giourntas, T. Hodgkiess, and A. M. Galloway, "Comparative study of erosion–corrosion performance on a range of stainless steels," *Wear*, vol. 332–333, pp. 1051–1058, 2015.

[6] M. Jones and R. J. Llewellyn, "Assessing the Erosion Corrosion Properties of Materials for Slurry transportation and processing in the oil sands industry," *Nace Int. Corros. 2007 Conf. expo*, no. 07685, pp. 1–15.

[7] U. Malayoglu and A. Neville, "Mo and W as alloying elements in Co-based alloys—their effects on erosion–corrosion resistance," *Wear*, vol. 259, no. 1–6, pp. 219–229, 2005.

[8] U. Malayoglu and A. Neville, "Comparing the performance of HIPed and Cast Stellite 6 alloy in liquid–solid slurries," *Wear*, vol. 255, no. 1–6, pp. 181–194, 2003.

[9] S. A. Romo, J. F. Santa, J. E. Giraldo, and A. Toro, "Cavitation and high-velocity slurry erosion resistance of welded Stellite 6 alloy," *Tribol. Int.*, vol. 47, pp. 16–24, 2012.

[10] Y. Zhao, F. Zhou, J. Yao, S. Dong, and N. Li, "Erosion–corrosion behavior and corrosion resistance

of AISI 316 stainless steel in flow jet impingement," *Wear*, vol. 328–329, pp. 464–474, 2015.
[11] G. T. Burstein and K. Sasaki, "Effect of impact angle on the slurry erosion–corrosion of 304L stainless steel," *Wear*, vol. 240, no. 1–2, pp. 80–94, 2000.
[12] N. Andrews, L. Giourntas, A. . Galloway, and A. Pearson, "Effect of impact angle on the slurry erosion-corrosion of Stellite 6 and SS316," *Wear*, vol. 320. pp. 143–151, 2014.
[13] D. A. López, J. P. Congote, J. R. Cano, A. Toro, and A. P. Tschiptschin, "Effect of particle velocity and impact angle on the corrosion–erosion of AISI 304 and AISI 420 stainless steels," *Wear*, vol. 259, no. 1–6, pp. 118–124, 2005.
[14] L. Giourntas, T. Hodgkiess, and A. M. Galloway, "Enhanced approach of assessing the corrosive wear of engineering materials under impingement," *Wear*, vol. 338–339, pp. 155–163, 2015.
[15] I. Finnie, "The mechanism of erosion of ductile metals," in *3rd U.S. Congr. Appl. Mechanics*, 1958.
[16] S. Aribo, R. Barker, X. Hu, and A. Neville, "Erosion–corrosion behaviour of lean duplex stainless steels in 3.5% NaCl solution," *Wear*, vol. 302, no. 1–2, pp. 1602–1608, 2013.
[17] A. N. J. Stevenson and I. M. Hutchings, "Wear of Hardfacing While Cast Irons By Solid Particle Erosion," *Wear*, vol. 186, no. 1, pp. 150–158, 1995.
[18] R. J. Llewellyn, S. K. Yick, and K. F. Dolman, "Scouring erosion resistance of metallic materials used in slurry pump service," *Wear*, vol. 256, no. 6, pp. 592–599, 2004.